Supplementary Material – Revealing Hund's multiplets in Mott insulators under strong electric fields

Nagamalleswararao Dasari,[1] Jiajun Li,[1] Philipp Werner,[2] and Martin Eckstein[1]

[1] *Department of Physics, University of Erlangen-Nuremberg, 91058 Erlangen, Germany*
[2] *Department of Physics, University of Fribourg, 1700 Fribourg, Switzerland*

(Dated: March 20, 2020)

Method

We employ the real-time Dynamical mean-field theory (DMFT) to solve the two-band Hubbard model. The DMFT formalism neglects the momentum dependence of the self-energy $\Sigma_k(t,t') \approx \Sigma(t,t')$, which allows to map the lattice model [Eq. (1) in the main text] to an impurity action[1, 2]

$$S = -i\int_C dt H^{\rm loc}(t) - i\int_C dt dt' \sum_{\sigma,l,l'} \hat{c}^\dagger_{l\sigma}(t)\hat{\Delta}_{l,l'}(t,t')\hat{c}_{l'\sigma}(t')$$

with self-consistently determined hybridization function $\hat{\Delta}_{l,l'}(t,t')$. The Bethe lattice self-consistency condition under the electric field is given by[3]

$$\hat{\Delta}_\sigma(t,t') = \frac{1}{6}\sum_{\alpha=x,y,z,\zeta=\pm} e^{i\zeta\phi_\alpha}\hat{T}^{\alpha\dagger}\hat{G}_\sigma\hat{T}^\alpha e^{-i\zeta\phi_\alpha} \equiv \Delta_+ + \Delta_-$$

where quantities with a hat are 2×2 matrices in orbital space. The above self-consistency condition represents a Bethe lattice in which d bonds are connected to each lattice site along the three directions $\alpha = x, y, z$. The hopping matrices along the three directions are given by

$$T_x = \frac{1}{4}\begin{pmatrix} 3 & -\sqrt{3} \\ -\sqrt{3} & 1 \end{pmatrix}, T_y = \frac{1}{4}\begin{pmatrix} 3 & \sqrt{3} \\ \sqrt{3} & 1 \end{pmatrix}, T_z = \begin{pmatrix} 0 & 0 \\ 0 & 1 \end{pmatrix}.$$

Furthermore, ϕ_α is the Peierls phase along the bond direction α. For each direction there are bonds pointing along ($\zeta = +1$) and against ($\zeta = -1$) the external field, and the corresponding contributions to the hybridization function are denoted by $\hat{\Delta}_+$ ($\hat{\Delta}_-$). The multi-orbital version of the non-crossing approximation (NCA) is used to calculate the impurity self-energy $\hat{\Sigma}(t,t')$[4]. Real-time DMFT measures the local Green's function $\hat{G}$ from which the electric current can be calculated. The expression for the electric current is $j(t) = {\rm Im}\big(\Gamma_+ - \Gamma_-\big)$ where $\Gamma_{+/-} = -i{\rm Tr}[\hat{\Delta}_{+/-} * \hat{G}]^<(t,t)$.

Current resonances

In this section we analyze the current and excitation density in the regime of strong fields, where near resonances $U = nE_0$ are expected to play a role. Figure 1 shows the current (averaged over the time-interval $25 < t < 35$), for the same setting as Fig. (1) in the main text. After an exponential increase of the current for small electric fields $E_0 \lesssim 1$ (i.e., the dielectric breakdown analyzed in the main text), the current becomes highly non-linear with sharp resonance peaks. For $J = 0$ (Fig. 1), the strongest visible resonances appear around $E_0 = U/2, U/3, U/4, 2U/3$ (the resonance $E_0 = U$ is not visible here, because the system is so rapidly excited that for $25 < t < 35$ the current has already decayed). For $J > 0$, all resonances broaden and eventually merge into a continuum. The broadening is simply understood because for $J > 0$ resonances may appear at least at all combinations $E_0 = (U + J)/n$, $E_0 = (U - J)/n$, $E_0 = (U - 3J)/n$, and are thus no longer individually resolved.

In order to better resolve the effect of J on the resonant excitation, it is slightly better to look at the total double occupancy at the impurity at a given time $t = 35$ after the excitation (Fig. 2). At least for the fields close to $E_0 = (U+J)/2, (U-J)/2, (U-3J)/2$ an enhancement of the excitation is visible (arrows in Fig. 2b and c). Furthermore, one can resolve the individual contributions of the three multiplet occupations $|\uparrow,\uparrow\rangle$ (high-spin state), $|\uparrow,\downarrow\rangle$ (inter-orbital singlet), and $|\uparrow\downarrow,0\rangle$ (intra-orbital doublon) to the double occupancy. When $J = 0$, due to the degeneracy of the atomic ground state, each spin sector contributes equally to the net excitation density of doublons. But for any finite J they contribute differently to the net value, and the resonance peaks in each spin sector occur at different field strengths. For example, the single peak in Fig. 2a) at $E_0 = U/2 = 4$ splits into three different peaks for any finite J, where a maximum of $\Delta_{|\uparrow,\uparrow\rangle}$ occurs around $E_0 = (U + J)/2$, a maximum of $\Delta_{|\uparrow,\downarrow\rangle}$ occurs around $E_0 = (U - J)/2$, and a maximum of $\Delta_{|\uparrow\downarrow,0\rangle}$ occurs around $E_0 = (U - 3J)/2$.

[1] J. K. Freericks, V. M. Turkowski, and V. Zlatić, Phys. Rev. Lett. **97**, 266408 (2006).
[2] H. Aoki, N. Tsuji, M. Eckstein, M. Kollar, T. Oka, and P. Werner, Rev. Mod. Phys. **86**, 779 (2014).
[3] J. Li, H. U. R. Strand, P. Werner, and M. Eckstein, Nature Communications **9**, 4581 (2018).
[4] M. Eckstein and P. Werner, Phys. Rev. B **82**, 115115 (2010).

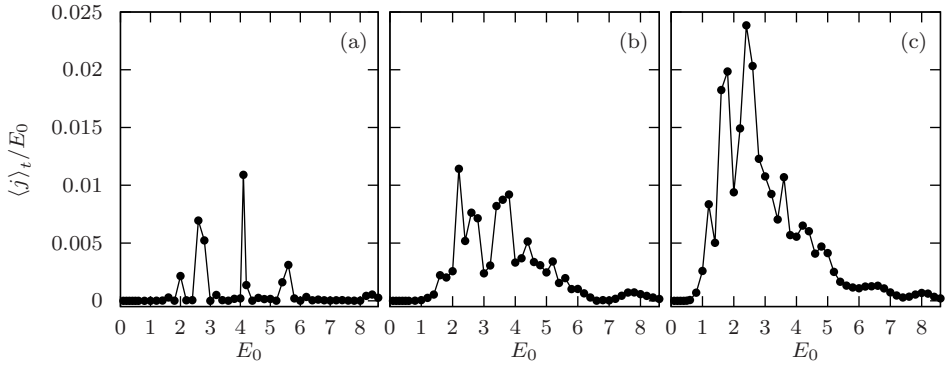

FIG. 1. Current averaged over time $25 < t < 35$, as a function of the field E_0 for $J =$ (a) 0.0 (b) 0.48 (c) 0.96. The interaction is $U = 8$.

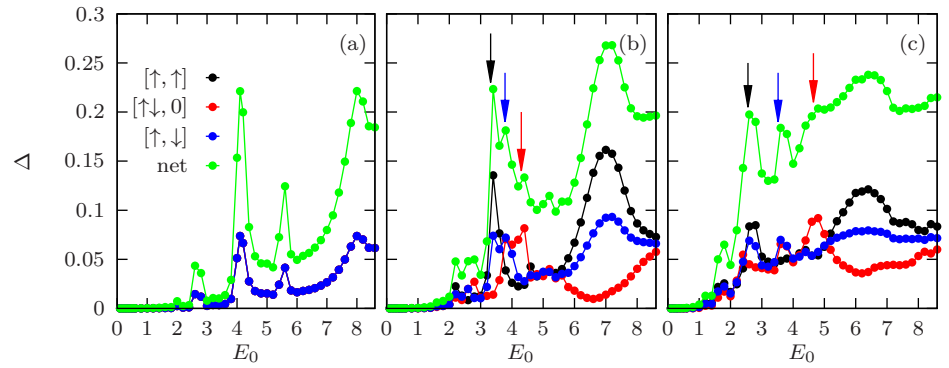

FIG. 2. Excitation density of doublons in different spin sectors for J is (a) 0.0 (b) 0.48 (c) 0.96. Here $\Delta_a = d_a(t = 35) - d_a(t = 0)$ is the difference between excited state and equilibrium occupation of the states $a = |\uparrow,\uparrow\rangle$ (high-spin state), $|\uparrow,\downarrow\rangle$ (inter-orbital singlet), and $|\uparrow\downarrow, 0\rangle$ (intra-orbital doublon). The green curve indicates the total excitation density of doublons, and arrows show the position of the resonances, $E_0 = (U + J)/2, (U - J)/2, (U - 3J)/2$.